

This discussion paper is/has been under review for the journal Biogeosciences (BG).
Please refer to the corresponding final paper in BG if available.

Parameter-induced uncertainty quantification of soil N₂O, NO and CO₂ emission from Höglwald spruce forest (Germany) using the LandscapeDNDC model

K.-H. Rahn¹, C. Werner^{1,*}, R. Kiese¹, E. Haas¹, and K. Butterbach-Bahl¹

¹Karlsruhe Institute of Technology, Institute for Meteorology and Climate Research, Atmospheric Environmental Research, Kreuzeckbahnstr. 19, 82467 Garmisch-Partenkirchen, Germany

*now at: Biodiversity and Climate Research Centre (BIK-F), Senckenberg Gesellschaft für Naturforschung, Senckenberganlage 25, 60325 Frankfurt am Main, Germany

Received: 14 February 2012 – Accepted: 11 April 2012 – Published: 27 April 2012

Correspondence to: R. Kiese (ralf.kiese@kit.edu)

Published by Copernicus Publications on behalf of the European Geosciences Union.

BGD

9, 5249–5286, 2012

UQ of soil GHG emissions using LandscapeDNDC

K.-H. Rahn et al.

Title Page

Abstract

Introduction

Conclusions

References

Tables

Figures

◀

▶

◀

▶

Back

Close

Full Screen / Esc

Printer-friendly Version

Interactive Discussion



Abstract

Assessing the uncertainties of simulation results of ecological models is becoming of increasing importance, specifically if these models are used to estimate greenhouse gas emissions at site to regional/national levels. Four general sources of uncertainty effect the outcome of process-based models: (i) uncertainty of information used to initialise and drive the model, (ii) uncertainty of model parameters describing specific ecosystem processes, (iii) uncertainty of the model structure and (iv) accurateness of measurements (e.g. soil-atmosphere greenhouse gas exchange) which are used for model testing and development.

The aim of our study was to assess the simulation uncertainty of the process-based biogeochemical model LandscapeDNDC. For this we set up a Bayesian framework using a Markov Chain Monte Carlo (MCMC) method, to estimate the joint model parameter distribution. Data for model testing, parameter estimation and uncertainty assessment were taken from observations of soil fluxes of nitrous oxide (N_2O), nitric oxide (NO), and carbon dioxide (CO_2) as observed over a 10 yr period at the spruce site of the Hoglwald Forest, Germany. By running four independent Markov Chains in parallel with identical properties (except for the parameter start values), an objective criteria for chain convergence developed by Gelman et al. (2003) could be used.

Our approach showed that by means of the joined parameter distribution, we were able not only to limit the parameter space and specify the probability of parameter values, but also to assess the complex dependencies among model parameters used for simulating soil C and N trace gas emissions. This helped to improve the understanding of the behaviour of the complex LandscapeDNDC model while simulating soil C and N turnover processes and associated C and N soil-atmosphere exchange.

In a final step the parameter distribution of the most sensitive parameters determining soil-atmosphere C and N exchange were used to obtain the parameter-induced uncertainty of simulated N_2O , NO and CO_2 emissions. These were compared to observational data of the calibration set (6 yr) and an independent validation set of 4 yr.

BGD

9, 5249–5286, 2012

UQ of soil GHG emissions using LandscapeDNDC

K.-H. Rahn et al.

Title Page

Abstract

Introduction

Conclusions

References

Tables

Figures

◀

▶

◀

▶

Back

Close

Full Screen / Esc

Printer-friendly Version

Interactive Discussion



The comparison showed that most of the annual observed trace gas emissions were in the range of simulated values and were predicted with a high certainty (Residual mean squared error (RMSE) NO: 2.5 to 21.3 gNha⁻¹ d⁻¹, N₂O: 0.2 to 21.4 gNha⁻¹ d⁻¹, CO₂: 5.8 to 12.6 kgCha⁻¹ d⁻¹). However, LandscapeDNDC simulations were sometimes limited to accurately predict observed seasonal variations in fluxes.

1 Introduction

Trace gas emissions (N₂O, NO and CO₂) from soils of terrestrial ecosystems are highly variable in space and time due to the interplay of climatic drivers (mainly rainfall and temperature) and various ecosystem processes involved in C and N transformation and associated formation of trace gases. Therefore, quantification of the annual sink or source strength of soil greenhouse gases (GHG) is still a challenge. For sound estimates at site scale, measurements are labour and cost intensive since they should be carried out at high temporal scale covering full annual cycles (Kiese et al., 2005; Werner et al., 2006). For that reason quantification of soil GHG emission on regional/national scale cannot solely depend on measurements but need to follow a joint measuring and modelling approach. In recent years an increasing number of biogeochemical models were tested on site scale and after sound validation were applied in a coupled GIS model approach for regionalization of soil GHG emissions (Del Grosso et al., 2006; Kesik et al., 2006; Pathak et al., 2005; Li et al., 2004; Salas et al., 2007; Potter et al., 1996; Butterbach-Bahl et al., 2001; Kiese et al., 2005). This approach is in line with the IPCC recommendations and requirements to develop improved inventories by use of biogeochemical models. However, the so-called Tier 3 approach includes not only up-scaling of GHG emissions but also the obligation to perform uncertainty quantification of the simulation results.

Uncertainty of model predictions can be classified into four categories: (i) uncertainty of information used to initialise and drive the model (Vrugt et al., 2008; Wikle, 2003), (ii) uncertainty of model parameters (e.g. describing specific ecosystem processes)

UQ of soil GHG emissions using LandscapeDNDC

K.-H. Rahn et al.

Title Page

Abstract

Introduction

Conclusions

References

Tables

Figures

◀

▶

◀

▶

Back

Close

Full Screen / Esc

Printer-friendly Version

Interactive Discussion



(Vrugt et al., 2003), (iii) uncertainty of the model structure (Refsgaard et al., 2006) and (iv) accurateness of measurements (e.g. soil-atmosphere greenhouse gas exchange), which are used for model improvement and development (e.g., van Oijen et al., 2005). Uncertainty estimates in many studies investigating the soil-atmosphere exchange of trace gases only cover the assessment of uncertainty imposed by input data (e.g., Li et al., 2004; Werner et al., 2007; Winiwarter and Rypdal, 2001; Kiese et al., 2005). Due to the high complexity and large number of model parameters, work focused less on uncertainty related to model parameters as the computational demand of complex models is high and often model adaptations are required to allow application of statistical methods.

In recent years the Bayesian approach was increasingly used to quantify model parameter uncertainty on simulation results of process-based models. The Bayesian theorem was used for calibration and uncertainty assessment of parameters of dynamic process-based forest models mainly focusing on carbon turnover (van Oijen et al., 2005; Svensson et al., 2008; Klemmedtsson et al., 2008) and more recently also for parameters involved in production, consumption, transport and emissions of soil GHGs (e.g., Lehuger et al., 2009). To our knowledge van Oijen et al. (2011) is the only study so far comparing four process-based biogeochemical forest models within a Bayesian model comparison framework. In contrast to such a model inter-comparison, the aim of this study is to provide deeper insights into the individual parameter uncertainty and calibration of the model LandscapeDNDC and the subsequent uncertainty of simulated trace gas exchange. The parameter distribution, which was estimated after an objective multi-chain convergence check, was additionally tested on a validation dataset.

LandscapeDNDC is a process-oriented biogeochemical model, which simulates the biosphere-atmosphere exchange of greenhouse gases on basis of the simulation of all major ecosystem C and N cycling processes, thereby considering (a) microbial processes (e.g. immobilisation, nitrification, denitrification), (b) plant processes (e.g., photosynthesis, respiration, N-immobilisation, litter fall) as well as (c) a series of

BGD

9, 5249–5286, 2012

UQ of soil GHG emissions using LandscapeDNDC

K.-H. Rahn et al.

Title Page

Abstract

Introduction

Conclusions

References

Tables

Figures

◀

▶

◀

▶

Back

Close

Full Screen / Esc

Printer-friendly Version

Interactive Discussion



physico-chemical processes (e.g. gas diffusion, water movement in soils) (Butterbach-Bahl et al., 2004; Li et al., 2001; Grote et al., 2009, 2011; Haas et al., 2012).

We used a time series covering 10 yr of soil-atmosphere trace gas fluxes as observed continuously in sub-daily time resolution at the Höglwald spruce forest, Germany (e.g., Butterbach-Bahl et al., 2002; Wu et al., 2010), to assess the model parameter uncertainty of the LandscapeDNDC model.

Results of the Bayesian calibration approach can be used to gain insights into the complex parameter dependencies, to identify weaknesses in process descriptions and to narrow the range of likely parameter values of the model, which finally reduces uncertainty of the simulation results.

2 Model description and model parameter selection

The LandscapeDNDC model applied in this study is a derivative of the DNDC model family further developed at IMK-IFU Garmisch-Partenkirchen, Germany. LandscapeDNDC was developed from DNDC (agricultural sites) and PnET-N-DNDC/Forest-DNDC (forest sites), which were initially set up to predict soil carbon and nitrogen biogeochemistry, with a specific focus on the simulation of soil N trace gas emissions (Li et al., 2000; Stange et al., 2000; Butterbach-Bahl et al., 2001; Kiese et al., 2005; Kesik et al., 2005; Werner et al., 2007).

LandscapeDNDC integrates different modules for describing soil environmental conditions (temperature, moisture, pH, nutrient availability and anaerobic volume fractions), soil-chemistry integrating microbial C and N turnover processes (mineralisation, nitrification and denitrification) and associated C and N trace gas emissions (e.g. N₂O, NO and CO₂) as well as vegetation dynamics (nutrient uptake, growth and litterfall).

Each module includes parameters derived from physical and chemical principals and laboratory measurements. In this study we focus on the analysis of parameter-induced uncertainty quantification stemming from the soil-chemistry module describing all processes relevant for C and N trace gas production, consumption and transport,

Title Page

Abstract

Introduction

Conclusions

References

Tables

Figures



Back

Close

Full Screen / Esc

Printer-friendly Version

Interactive Discussion



being crucial for the simulation of soil GHG emissions. Here, we do not consider model parameters for the plant growth and soil water cycling modules in order to reduce complexity and degrees of freedom and increase efficiency of the calibration process.

The soil-chemistry sub-module in total holds 67 parameters, mostly describing biological kinetics of nutrient turnover and transformation by growth and death of different types of microbes (e.g. nitrifiers and denitrifiers). Parameter values are generally derived from laboratory measurements and expert knowledge, if detailed information is not available. This introduces different levels of uncertainty, which need to be quantified and requires calibration.

The model parameters can only be estimated and optimised by an inverse calibration technique (cf. Vrugt et al., 2003), which compares model simulation output by using randomly selected model parameter vectors with measured observations. The observational data used was collected at the Höglwald spruce forest, Germany, covering the years 1994 to 1997 and 2002 to 2003 (Papen and Butterbach-Bahl, 1999; Gasche and Papen, 1999). The remaining observation period (years 2004 to 2007) was used for validation purpose and finally for assessing the prediction uncertainty.

Each parameter included into the uncertainty analysis adds a new dimension in the parameter space. Therefore, computational cost rises tremendously with the increasing number of parameters while efficiency of the calibration technique decreases. Furthermore, correlations among parameters become more likely by increasing the number of parameters. This subsequently leads to slower convergence rates (requiring additional iterations), as only parameter vectors which comply with these relations are accepted by the Bayesian algorithm (cf. Gilks et al., 1996). Additionally, more degrees of freedom exist, i.e. parameter configurations producing similar outputs may not be unique. To avoid these obstacles we used a sensitivity analysis (Saltelli, 2008) developed by Morris (1991) prior to the Bayesian calibration method in order to restrict the analysis to the most influential parameters and to avoid over-fitting effects.

The method introduced by Morris is an efficient tool for parameter screening, since it can easily be implemented and computational demands are low (van Oijen et al.,

BGD

9, 5249–5286, 2012

UQ of soil GHG emissions using LandscapeDNDC

K.-H. Rahn et al.

Title Page

Abstract

Introduction

Conclusions

References

Tables

Figures

◀

▶

◀

▶

Back

Close

Full Screen / Esc

Printer-friendly Version

Interactive Discussion



2011). The method varies parameter values and finally produces a ranking of the model parameters based on their impact on the simulated model output of C and N trace gas emissions and soil moisture.

This procedure divides each parameter range in n (here $n = 6$) equidistant levels, starts with a random parameter vector using these levels and randomly changes one parameter after another to one of the other levels (1 iteration). Differences in model output are stored and used to rank the model parameters according to their influence on the simulation output. Since the trajectory of parameter changes per iteration is randomly selected m times (here $m = 5000$), the method spans the parameter space better than a “one-parameter-at-a-time approach” (see Hamby, 1994). The model parameters, which produce largest differences (i.e. having highest sensitivity on the output variable), are regarded as the most influential ones.

To identify the most sensitive parameters of LandscapeDNDC affecting soil C and N fluxes we initialised and run the model with specific site information (soil, vegetation and climate) of the Höglwald spruce forest. This approach does not require a comparison of simulated emission to measurements, since the sensitivity analysis only focuses on parameter-induced changes of model output. Parameter sensitivities were calculated separately for the output variables of soil N₂O, NO and CO₂ emissions, which finally resulted in three different parameter-ranking lists. We selected the first 20 most influential parameters of any list, thereby considering the trade-off between over-parameterisation and under-representing significant processes. Due to close linkage of C and N cycling and in particular NO and N₂O emission there was a good overlap of the most sensitive parameters, which lead to a overall selection of 26 parameters (see Table 1).

For evaluation, whether the reduced parameter set accounts for most of the models behaviour, we regressed the stored model output (a) to all parameters and (b) to the reduced parameter subset and compared the adjusted coefficient of determination \bar{R}^2 of both linear regressions (cf. van Oijen et al., 2011). The results show that for N₂O and CO₂ more than 90% of the models behaviour is explained by the subset of the parameters. The behaviour of NO simulations is explained by 65% using the subset.

UQ of soil GHG emissions using LandscapeDNDC

K.-H. Rahn et al.

Title Page

Abstract

Introduction

Conclusions

References

Tables

Figures

◀

▶

◀

▶

Back

Close

Full Screen / Esc

Printer-friendly Version

Interactive Discussion



We regard these numbers to be sufficient for continuing the Bayesian calibration approach with the restricted parameter set and at the same time assure a balance with calibration efficiency, which will be reduced when introducing more parameters as already stated before. Following the selection of the most sensitive model parameters, the joined parameter distribution given the data was estimated by means of a Bayesian calibration. From this distribution parameter values can be sampled to perform simulation runs and finally address the frequency distribution of simulation results. See Fig. 1 for an illustration of the workflow.

3 Bayesian calibration

In a standard frequency approach the parameter value is not regarded as a random variable. The used parameter value is either the true value or it is not (see Ellison, 1996). Therefore, a Bayesian approach is needed (Clark, 2005; van Oijen et al., 2005; Klemedtsson et al., 2008; Gelman et al., 2003; Reinds et al., 2008; Lehuger et al., 2009) since it models the parameter vector θ as a random vector, which allows a direct quantification of the probability of a certain parameter realisation/range.

The probability density of a parameter value given the measurement D (posterior) is:

$$p(\theta|D). \quad (1)$$

By using Bayes theorem, the posterior is proportional to the product of the likelihood $p(D|\theta)$ and the prior density $p(\theta)$:

$$p(\theta|D) \propto p(D|\theta) \cdot p(\theta). \quad (2)$$

The prior, describing the a priori knowledge on parameters, is determined by using literature data and biogeochemical principles to address the most likely parameter value and to constrain the range of a parameter. We use an uninformed prior (uniform distribution) ranging between provided minima and maxima for the given parameter as

BGD

9, 5249–5286, 2012

UQ of soil GHG emissions using LandscapeDNDC

K.-H. Rahn et al.

Title Page

Abstract

Introduction

Conclusions

References

Tables

Figures

◀

▶

◀

▶

Back

Close

Full Screen / Esc

Printer-friendly Version

Interactive Discussion



derived from expert knowledge or laboratory and field experiments. The likelihood, the only unknown term, describes the probability of a data realisation for a particular parameter vector.

We assume the error $D - M$ between data D and model M to be normal distributed, hence the likelihood is (van Oijen et al., 2005):

$$p(D|\theta) = \frac{1}{\sqrt{2\pi\sigma}} e^{-\frac{(D-M(\theta))^2}{2\sigma^2}} \quad (3)$$

Since this term cannot be solved analytically, a Metropolis algorithm (Metropolis et al., 1953) generates a Markov chain, which samples from the posterior distribution after convergence of the chain (see next section for convergence criteria).

Although the model produces results on a daily time-step, simulations and measurements were aggregated to weekly means to avoid that minor temporal lags between measured data and model simulations penalise likelihood calculations. A further aggregation of data to e.g. monthly means, however, results in a significant loss of seasonal dynamics of trace gas fluxes and was thus not applied here.

In order to increase computation efficiency, we run the model in parallel for the six simulated calibration years on a High Performance Computing (HPC) Linux cluster.

3.1 Criteria to define convergence while using a multi-chain approach

As it is not possible to draw any statistical inference from the sampled parameter vectors if the Markov chain has not converged (Gilks et al., 1996), we used four independent Markov chains (differing only in the individual parameter starting points) and tested for convergence at each iteration step. When convergence was reached (end of “burn in phase”), the previous parameter samples were discarded and all following data were included in the further analysis.

To quantify convergence, Gelman et al. (2003) introduced the measure \hat{R} which compares the variances of each chain (within sequence variance, Eq. 4) to the joined

[Title Page](#)[Abstract](#)[Introduction](#)[Conclusions](#)[References](#)[Tables](#)[Figures](#)[◀](#)[▶](#)[◀](#)[▶](#)[Back](#)[Close](#)[Full Screen / Esc](#)[Printer-friendly Version](#)[Interactive Discussion](#)

variance of all chains (between sequence variance, Eq. 5)

$$W = \frac{1}{m} \sum_{j=1}^m s_j^2, \text{ where } s_j^2 = \frac{1}{n-1} \sum_{i=1}^n (\psi_{i,j} - \bar{\psi}_{\cdot,j})^2 \quad (4)$$

$$B = \frac{n}{m-1} \sum_{j=1}^m (\bar{\psi}_{\cdot,j} - \bar{\psi}_{\cdot\cdot})^2, \text{ where } \bar{\psi}_{\cdot,j} = \frac{1}{n} \sum_{i=1}^n \psi_{i,j}, \bar{\psi}_{\cdot\cdot} = \frac{1}{m} \sum_{j=1}^m \bar{\psi}_{\cdot,j}. \quad (5)$$

In the process of convergence the measure $\hat{R} = \sqrt{\frac{n-1}{n} + \frac{B}{nW}}$ approaches from values > 1.0 to 1.0. As \hat{R} is not expected to reach exactly 1.0, a threshold of 1.2 is introduced as the acceptance threshold (Kass et al., 1998).

By using four chains, our implementation spreads the model to 24 CPUs (4 chains × 6 separate simulation years) using the Message Passing Interface (MPI). After 1000 iteration steps the Gelman/Rubin statistic was calculated and continuously updated until convergence (according to \hat{R}) of chains. In our setup, burn-in of all parameters was completed after 31 656 iteration steps. Following convergence, 50 000 additional iterations were sampled for each chain, which resulted in a total of 200 000 samples from the posterior distribution.

The acceptance-rates of the four chains ranged from 13% to 17% (using a step-width of 0.04). These are reasonable values taking into account the large dataset (6 yr of data in daily time resolution and 4 target variables: CO₂, N₂O, NO and water content) and therefore a rather strict rejection step due to a narrow shaped posterior (Arhonditsis et al., 2008; Clark, 2005; Rahn et al., 2011).

3.2 Effective data storage

The study design and computational setup lead to substantial amounts of data, which need to be efficiently handled within subsequent data analysis. For that reason a

Title Page

Abstract

Introduction

Conclusions

References

Tables

Figures

◀

▶

◀

▶

Back

Close

Full Screen / Esc

Printer-friendly Version

Interactive Discussion



interface to a relational database was developed using structured query language (SQL) which warranted a concurrent access and high data integrity.

4 Estimating simulated gas flux distributions

In a second step the posterior distribution of the 26 parameters was used to quantify the uncertainty of LandscapeDNDC simulations for soil N₂O, NO and CO₂ emissions of the Höglwald Forest spruce site (see Fig. 1). For this, we used a total of 20 000 posterior-parameter vectors (posterior-samples) by selecting every 10th parameter vector out of the 200 000 posterior-parameter samples of the four chains (50 000 for each chain). Thereby, we reduced dependencies between parameter vectors of consecutive iterations (Kass et al., 1998; Toft et al., 2007), which arose as each parameter vector of the posterior distribution had been taken dependent on its predecessor during the calibration process.

Following the selection of the posterior-samples, we executed LandscapeDNDC with the parameter realisations for the calibration set (years 1994 to 1997 and 2002 to 2003) and an independent validation data set (years 2004 to 2007). As a result we obtained distributions (including associated uncertainty) of simulated soil N₂O, NO and CO₂ emissions.

The residual mean squared error (RMSE) is used to quantify the error between measurements and simulations. Therefore, we defined the distance of measurements to the distribution of the simulations as the minimum of the distances between the measurements and the two boundaries of the credible interval or 0 whenever the measurement is within the range of the credible interval. The RMSE of the best simulation (RMSE(θ_{MAP})) is calculated using the common definition.

BGD

9, 5249–5286, 2012

UQ of soil GHG emissions using LandscapeDNDC

K.-H. Rahn et al.

Title Page

Abstract

Introduction

Conclusions

References

Tables

Figures

◀

▶

◀

▶

Back

Close

Full Screen / Esc

Printer-friendly Version

Interactive Discussion



5 Results

5.1 Posterior parameter distribution

An estimate for the posterior distribution of the 26 most sensitive LandscapeDNDC parameters for simulation of soil N₂O, NO and CO₂ emissions was obtained by using Bayesian calibration technique and initial information on the likely range of the selected parameters. To illustrate common features of the obtained marginal posterior distributions, we present a subset of four model parameters (see Fig. 4 and Table 2). For each marginal histogram, 4 × 50 000 post burn-in chain steps were used.

In the first histogram (Fig. 4a) the marginal distribution of the parameter KN2O, the loss rate of N₂O during nitrification, is displayed. The prior parameter uncertainty ($SD_{\text{prior}} = 0.026$) was reduced substantially ($SD_{\text{post}} = 0.006$) and the most probable value of the right skewed distribution is in a narrow region between 0.002 and 0.008.

Figure 4b shows a bimodal distribution for the parameter EFFAC, i.e. the parameter describing the partitioning of CO₂ and DOC production during microbial decomposition of organic matter. As a result of the calibration procedure EFFAC has two regions of “attraction” separated by a region, which is less probable (lower posterior values). For bimodal distributions it is difficult for the metropolis algorithm to traverse from one mode of the parameter space to the other (cf. Vrugt et al., 2009). Therefore, the convergence rate, which describes how fast the chains converge to the posterior distribution, is lower. Two of the four chains (red and blue lines) sample from both modes, whereas the other two (yellow and green lines) are still taking most of the samples from only one mode. Although the Gelman/Rubin Statistics indicated a converged chain, the plots indicate, that the calculation procedure still would need to continue well beyond the achieved runs to reach a true convergence. Nevertheless, as samples from four chains are available, which almost all support the two modes, the number of samples is sufficient to approximate the full bimodal distribution of the parameter EFFAC.

Figure 4c displays the posterior distribution of the parameter KHDC_L. This parameter is the decomposition constant for the labile humads pool (death microbial biomass).

BGD

9, 5249–5286, 2012

UQ of soil GHG emissions using LandscapeDNDC

K.-H. Rahn et al.

Title Page

Abstract

Introduction

Conclusions

References

Tables

Figures

◀

▶

◀

▶

Back

Close

Full Screen / Esc

Printer-friendly Version

Interactive Discussion



For this model parameter the posterior distribution is flat, i.e. all values across the explored range are of similar probability. Here, the uncertainty of the initial parameter could not be reduced significantly by the Bayesian calibration and only values approaching zero are less likely than others.

5 An example for a left skewed distribution of a parameter is given in Fig. 4d, in this case of KRCL. KRCL is the decomposition constant for the labile litter pool. Although there is a tendency for higher values, smaller values can still occur depending on the values of the other 25 parameters. In conclusion, the uncertainty of the parameter KRCL is reduced, however, not as much as compared to KN2O.

10 A correlation analysis between the 26 selected parameters revealed for most pairwise constellations no relevant correlations. This is due to the large number of sampling points in the entire parameter space (see Fig. 9. Higher correlations in absolute appeared only between KMNO2 (Michaelis-Menten constant for NO₂ to NO₃ during heterotrophic nitrification) and DRF (scaling factor for decomposition rate constants of SOM) with a correlation of -0.62, between EFFAC and D.N2O with 0.48, and between EFFAC and FNO3_U (fraction of microbial N-uptake as NO₃) with 0.46. All other correlations were in the range of ±0.40, most of them between ±0.25 (Fig. 8).

15 However, that does not fully exclude any relationship between parameters, since they are often of non-linear character. Figure 2 shows that limiting the values of EFFAC to values < 0.5 leads to a bell shaped distribution of the parameter DRF (scaling factor for decomposition rate constants of SOM) around the value 0.035 (correlation between EFFAC/DRF = 0.25). At the same time smaller values of FTRANS (factor regulating microbial nitrate immobilisation and direct re-mineralisation to NH₄), FNO3_U, KRCL (decomposition constant for recalcitrant litter pool) and KMM_DOC (Michaelis-Menten constant regulating growth of microbes in dependency of DOC substrate) become more likely, whereas for other parameters like MICRRESP (factor regulating CO₂ production during microbial metabolism in dependency of microbial C/N ratio), FRC (factor regulating microbial death depending on the availability of very labile and labile carbon) and KN2O (loss rate of N₂O during nitrification) higher values occur more often, thus get

UQ of soil GHG emissions using LandscapeDNDC

K.-H. Rahn et al.

Title Page

Abstract

Introduction

Conclusions

References

Tables

Figures

◀

▶

◀

▶

Back

Close

Full Screen / Esc

Printer-friendly Version

Interactive Discussion



more likely. That also shows that restricting some parameters to a range of their most likely values can narrow the range of likely values of other parameters.

The heat map in Fig. 3, shows the relationship between KRCL and KMDC_N. While the correlation between the two parameters is low ($= -0.03$), one can see that lower values of KRCL restrict the range of KMDC_N to lower values. To capture all dependencies (compare Fig. 9) when estimating the distribution of model simulations, it is straightforward to use samples of the joined posterior parameter distribution, as the whole structure of parameter dependence is fully included.

5.2 Uncertainty quantification of soil atmosphere gas emissions at Höglwald forest (1994 to 1997, 2002 to 2003 and 2004 to 2007)

5.2.1 Calibration-set

In general, most of measured trace gas emissions of N_2O , NO and CO_2 are within or close to the range of the simulated 99 % credible interval (cf. Gilks et al., 1996) (see for example Fig. 5. RMSE values for each year and each soil-atmosphere flux are presented in Table 4). Based on the evaluation criteria, LandscapeDNDC was able to correctly simulate cumulative N_2O and NO emissions in five and four out of six years, respectively (see Table 3). In two out of three years, cumulative CO_2 observations were located within the simulated CO_2 ranges. Comparatively high NO emissions ($> 60 gNha^{-1}d^{-1}$) measured in the summers of 1996 and 2003, however, could not be reproduced by LandscapeDNDC (model simulations underestimated fluxes in summer periods by at least 29 % and 32 %, respectively).

Seasonal dynamics of NO measurements were reproduced for the years 1994, 1997 and partly for 2002, which resulted in low RMSE values for the credible interval (RMSE(CI): 2.46 to 3.18 $gNha^{-1}d^{-1}$) and when using the maximum posterior parameter vector θ_{MAP} (RMSE(θ_{MAP}): 6.66 to 9.20 $gNha^{-1}d^{-1}$). Although in most of the remaining years the magnitude of measurements and simulations is similar, the temporal dynamic could not always be clearly reproduced.

Title Page

Abstract

Introduction

Conclusions

References

Tables

Figures



Back

Close

Full Screen / Esc

Printer-friendly Version

Interactive Discussion



UQ of soil GHG emissions using LandscapeDNDC

K.-H. Rahn et al.

Title Page

Abstract

Introduction

Conclusions

References

Tables

Figures

◀

▶

◀

▶

Back

Close

Full Screen / Esc

Printer-friendly Version

Interactive Discussion



N_2O simulations especially suffer from the inability of the used model to simulate freeze-thaw pulse emissions (Papen and Butterbach-Bahl, 1999; Butterbach-Bahl et al., 2002; Wolf et al., 2010) in 1995, 1996, 1997 and 2003 (RMSE(CI): up to $16.54 \text{ g N ha}^{-1} \text{ d}^{-1}$). Therefore, following simulation to measurement comparisons of N_2O were restricted to periods being unaffected by freeze thaw events. Nevertheless, cumulative statistics and RMSE statistics can be compared with or without freeze thaw events in Tables 3 and 4. One can see that the RMSE is strongly reduced when neglecting frost-thaw emissions (e.g. RMSE(CI) reduced from 16.54 to 8.16 in 1996 and from 2.91 to 0.39 in 1997). Peak emissions of N_2O ($> 10 \text{ g N ha}^{-1} \text{ d}^{-1}$) in August 2002 could also not be reproduced by the model, although the model could comprehend the general increase of N_2O emissions in the beginning of August (up to $7 \text{ g N ha}^{-1} \text{ d}^{-1}$).

CO_2 emissions were underestimated by at least 22 % and 10 % during August to November in 1995 and 1996. From May to June 1997, they were overestimated by at least 31 %. Note that only 1004 CO_2 observations were used for calibration, compared to 1890 and 2075 values for NO and N_2O . Thus, CO_2 emissions were underweighted by a factor of approx. 0.5 in the calibration process.

5.2.2 Validation-set

To independently validate the behaviour of the parameterisation, we simulated soil atmosphere trace gas emissions in Höglwald for 2004 until 2007, i.e. to a time period, which has not been used for calibration of LandscapeDNDC. The parameterisation of the model includes the same posterior-samples that have been used to simulate the emissions of the calibration set (1994 to 1997, 2002 to 2003) and to visualise model uncertainty.

For the validation set, LandscapeDNDC produced comparable results as for the calibration set. Cumulative NO emissions were covered by the 99 % credible interval in three out of four simulated years but only in one year with regard to simulated N_2O emissions. Soil CO_2 emissions could be reproduced for all four years. Very low N_2O observations in 2004 were overestimated by at least 20 %, whereas measurements

were underestimated by 23 % in 2005 and 4 % in 2006 (excluding freeze-thaw events, which occurred in 2005 and 2006). Nevertheless, the averaged RMSE values of the validation set ($1.31 \text{ gNha}^{-1} \text{ d}^{-1}$) are not higher than the averaged RMSE values of the calibration set ($1.89 \text{ gNha}^{-1} \text{ d}^{-1}$).

5 The large discrepancy between soil NO simulations and measurements taken in 2006 (RMSE = $21.31 \text{ gNha}^{-1} \text{ d}^{-1}$) is the result of underestimated emissions from April to October (by at least 42 %).

Soil CO₂ fluxes were mainly overestimated during the periods May to July in 2005 (by 53 %), June to August in 2006 (by 62 %) and April to August in 2007 (by 85 %). Model shortcomings with regard to accurately simulate soil CO₂ fluxes during wintertime are obvious in 2005 and 2006 (see Fig. 6).

6 Discussion

Our work shows that the Bayesian calibration approach can successfully be implemented to estimate the posterior parameter distribution of a complex biogeochemical model used for simulating soil N₂O, NO and CO₂ fluxes at a spruce site of the Höglwald Forest, Germany. The applicability of the illustrated method to complex ecological models was also demonstrated in previous studies (e.g., van Oijen et al., 2005; Svensson et al., 2008; Klemmedtsson et al., 2008; Lehuger et al., 2009).

Bayesian calibration reduced the prior uncertainty (by up to 77 %) of 16 out of 26 parameters for simulating soil-atmosphere fluxes of the mentioned trace gases. For the remaining 10 parameters the calibration process achieved no significant reduction in parameter uncertainty. The flat shape of the distribution of these 10 parameters occurred because different parameter constellations can lead to similar model output. The underlying reasons for that cannot be further specified, as the parameter space is 26-dimensional and small changes in high-sensitive parameters may be compensated by changes of (many or all) remaining parameters.

UQ of soil GHG emissions using LandscapeDNDC

K.-H. Rahn et al.

Title Page

Abstract

Introduction

Conclusions

References

Tables

Figures



Back

Close

Full Screen / Esc

Printer-friendly Version

Interactive Discussion



UQ of soil GHG emissions using LandscapeDNDC

K.-H. Rahn et al.

Title Page

Abstract

Introduction

Conclusions

References

Tables

Figures

◀

▶

◀

▶

Back

Close

Full Screen / Esc

Printer-friendly Version

Interactive Discussion



Additionally, by simultaneously calibrating soil N_2O , NO and CO_2 emissions, we use a multi-objective (here three objectives) framework, so that a worsening of CO_2 estimation can be compensated by an improvement in NO or N_2O estimation. Gathering additional data (e.g. from different forests sites) may help to reduce uncertainty for these parameters. However, multiple parameter solutions do not affect the process of uncertainty estimation of soil-atmosphere gas fluxes modelled by LandscapeDNDC, as the posterior parameter solution is used (including all parameter constellations) to generate the distribution of simulated emissions.

The large number of parameters chosen, the complexity of the LandscapeDNDC model (simulating the entire C, N and water fluxes of terrestrial ecosystems), as well as a narrow shaped posterior distribution as a result of a detailed data-set (Arhonditsis et al., 2008; Rahn et al., 2011; Clark, 2005; van Oijen et al., 2011), reduces the acceptance-rate. Consequently, slow convergence rates of the chains were observed. The bimodal parameter EFFAC, which describes the partitioning of CO_2 and DOC production during microbial decomposition of organic matter, additionally hampers the algorithm to converge, as the parameter values have to pass a region of low probability to reach the other mode (cf. Vrugt et al., 2009). Therefore it took 31 656 samples until the chains converged and the additional 50 000 steps per chain required in total approximately three months computation time.

We could use the strength of an objective convergence check by using four independent chains. Thus, we are more secured of false conclusions using samples that were not (yet) drawn from the posterior distribution. The plot of the bimodal parameter EFFAC, however, shows that an overreliance on the value of the Gelman/Rubin statistic may also not be sufficient. Although the value of the statistic $\hat{R} < 1.2$ is indicating convergence of chains, the marginal distributions of each chain do not exactly follow the same shape. Nevertheless, as two chains show the bimodal shape and the other two sampled from one mode or the other mode, respectively, we can be convinced that the distribution including all 200 000 parameter values estimated the correct marginal posterior distribution also for this parameter.

The knowledge of all complex parameter dependencies helps to understand and improve the reliability of future model simulations and additionally to quantify the uncertainty of the simulated gas fluxes (N_2O , NO , CO_2) associated with model parameter uncertainty. As we use samples from the joined posterior distribution, we achieve more reliable uncertainty approximations of soil GHG exchange than by simply using samples of each marginal parameter distribution.

As we simultaneously calibrated the model parameters with data for three soil trace gas fluxes (N_2O , NO and CO_2) spanning six observation years, the parameter calibration results are a compromise for all years and the respective gas fluxes. Hence, better model simulation results are very likely to be obtained if single years or only one out of the three trace gases would have been chosen. Since the model is just an expert representation of the “real world” one cannot expect that simulation results and flux observations for all years and all gases are in perfect agreement. However, the results show that the LandscapeDNDC model is able to follow most of the dynamics as observed in field measurements and to approximate annual total emissions (see Table 3) with a certain accuracy (RMSE NO : 2.5 to 21.3 $\text{gNha}^{-1}\text{d}^{-1}$, N_2O : 0.2 to 21.4 $\text{gNha}^{-1}\text{d}^{-1}$, CO_2 : 5.8 to 12.6 $\text{kgCha}^{-1}\text{d}^{-1}$, Table 4) not only for the years which were used for model calibration but also for independent observation years.

Lowest agreement between measured and simulated fluxes was obtained for N_2O . Most of the discrepancy is due to the inability of LandscapeDNDC to simulate freeze-thaw N_2O pulse emission events. Since up to now no frost-thaw process descriptions were implemented into LandscapeDNDC, the calibration procedure was not able to fit the model to these fluxes sufficiently. At the Höglwald spruce site as well as in other temperate ecosystems exposed to severe winter freezing periods, freeze-thaw N_2O fluxes may dominate annual N_2O fluxes (Papen and Butterbach-Bahl, 1999; Wolf et al., 2010), so that a failure to simulate N_2O fluxes during freeze-thaw periods must lead to incorrect annual flux estimates. However, the comparison of N_2O data for the non-freeze-thaw periods shows, that simulations of N_2O fluxes by LandscapeDNDC are generally in the same range as the measurements for the calibration and at least

BGD

9, 5249–5286, 2012

UQ of soil GHG emissions using LandscapeDNDC

K.-H. Rahn et al.

Title Page

Abstract

Introduction

Conclusions

References

Tables

Figures

◀

▶

◀

▶

Back

Close

Full Screen / Esc

Printer-friendly Version

Interactive Discussion



close to measurements of the validation set. Nevertheless, due to the importance of freeze-thaw emissions for the annual N_2O budget there is an urgent need to further develop and implement model algorithms describing underlying processes of freeze-thaw based N_2O production and emission in/from soils (e.g., Wolf et al., 2011).

Also with regard to soil NO and CO_2 fluxes we identified short-comes of the used LandscapeDNDC. E.g. higher NO emissions in the summer period in 1995 and 1996 were systematically underestimated, while soil CO_2 emissions tended to be overestimated in the end of spring and beginning of summer and underestimated in subsequent summer days. This points either towards insufficient process descriptions, which have already been suggested earlier (Stange et al., 2000), or to problems with model initialisation. We limited the calibration procedure to a subset of 26 most influential parameters describing C and N turnover and production, consumption and emission processes of N_2O , NO and CO_2 in soils. To allow a more time efficient calibration, we excluded parameters describing soil water and vegetation dynamics. Nevertheless, the above-mentioned failures to accurately describe soil NO and CO_2 fluxes for all seasons point towards the necessity to recheck simulated soil water and vegetation dynamics in LandscapeDNDC.

However, in total the measurements of the calibration and the validation set were covered reasonably well (RMSE NO: 2.5 to 21.3 $\text{g N ha}^{-1} \text{d}^{-1}$, N_2O : 0.2 to 21.4 $\text{g N ha}^{-1} \text{d}^{-1}$, CO_2 : 5.8 to 12.6 $\text{kg C ha}^{-1} \text{d}^{-1}$, Table 4), in particular if we consider that we did not include all sources of errors (i.e. structural model error, input data error). In order to achieve improved approximations of the uncertainty of N_2O , NO and CO_2 emissions, a stochastic error term could be included in future research, e.g. by setting up a hierarchical Bayesian framework, to account for model miss-specifications (Rahn et al., 2011; Arhonditsis et al., 2008).

BGD

9, 5249–5286, 2012

UQ of soil GHG emissions using LandscapeDNDC

K.-H. Rahn et al.

Title Page

Abstract

Introduction

Conclusions

References

Tables

Figures

◀

▶

◀

▶

Back

Close

Full Screen / Esc

Printer-friendly Version

Interactive Discussion



7 Conclusions

Following the identification of the 26 most sensitive parameters out of a total of 67 model parameters describing soil emission of N_2O , NO and CO_2 in the biogeochemical model LandscapeDNDC, we successfully implemented a Bayesian calibration to estimate the joined posterior distribution of the most influential model parameters. To ensure that the posterior distribution of parameters was assessed, we used a multi-chain approach and tested for convergence of the Markov chain by the objective criteria developed by Gelman et al. (2003). In contrast to the a priori assumption of a uniform distribution of parameter values over a given range the posterior parameter distribution showed a more distinct pattern, including all complex parameter dependencies. Bayesian calibration reduced the prior uncertainty (by up to 77%) of 16 out of 26 parameters. This knowledge of the posterior probability distribution is of outstanding importance to guide future model development, e.g. to inform experimentalists which parameters need further investigation.

A comparison of simulated soil N_2O , NO and CO_2 emissions to measured flux data over the six observation years used in the calibration process showed high agreement. The same is true for independent validation data, including observations of four other years. Hence, we were able to quantify the parameter-induced uncertainty of the total simulated N_2O , NO and CO_2 emission. Furthermore, other uncertainty sources such as a model error need to be considered in order to estimate the total uncertainty of simulated soil fluxes of N_2O , NO and CO_2 .

In our study freeze-thaw events could not be reproduced, as underlying processes are not included in the LandscapeDNDC version used in this study. Since these events can potentially have a strong impact on the total annual soil N_2O emission, future model development and implementation of freeze-thaw algorithms is foreseen.

Acknowledgements. This work was part of the EU project NitroEurope, funded under the 6th EC Framework Programme for Research and Technological Development. This project received additional funding from the German Science Foundation (DFG) under contract no.

BGD

9, 5249–5286, 2012

UQ of soil GHG emissions using LandscapeDNDC

K.-H. Rahn et al.

Title Page

Abstract

Introduction

Conclusions

References

Tables

Figures

◀

▶

◀

▶

Back

Close

Full Screen / Esc

Printer-friendly Version

Interactive Discussion



BU1173/12-1. C. Werner would like to acknowledge financial support by the research funding program LOEWE “Landes-Offensive zur Entwicklung Wissenschaftlich-ökonomischer Exzellenz” of Hesse’s Ministry of Higher Education, Research, and the Arts.

References

- 5 Arhonditsis, G. B., Perhar, G., Zhang, W., Massos, E., Shi, M., and Das, A.: Addressing equifinality and uncertainty in eutrophication models, *Water Resour. Res.*, 44, W01420, doi:10.1029/2007WR005862, 2008. 5258, 5265, 5267
- Butterbach-Bahl, K., Stange, F., Papen, H., and Li, C.: Regional inventory of nitric oxide and nitrous oxide emissions for forest soils of southeast Germany using the biogeochemical model PnET-N-DNDC, *J. Geophys. Res.-Atmos.*, 106, 34155–34166, doi:10.1029/2000JD000173, 10 2001. 5251, 5253
- Butterbach-Bahl, K., Rothe, A., and Papen, H.: Effect of tree distance on N₂O and CH₄-fluxes from soils in temperate forest ecosystems, *Plant Soil*, 240, 91–103, doi:10.1023/A:1015828701885, 2002. 5253, 5263
- 15 Butterbach-Bahl, K., Kesik, M., Miehle, P., Papen, H., and Li, C.: Quantifying the regional source strength of N-trace gases across agricultural and forest ecosystems with process based models, *Plant Soil*, 260, 311–329, 2004. 5253
- Clark, J.: Why environmental scientists are becoming Bayesians, *Ecol. Lett.*, 8, 2–14, doi:10.1111/j.1461-0248.2004.00702.x, 2005. 5256, 5258, 5265
- 20 Del Grosso, S., Parton, W., Mosier, A., Walsh, M., Ojima, D., and Thornton, P.: DAYCENT national-scale simulations of nitrous oxide emissions from cropped soils in the United States, *J. Environ. Qual.*, 35, 1451–1460, 2006. 5251
- Ellison, A.: An introduction to Bayesian inference for ecological research and environmental decision-making, *Ecol. Appl.*, 6, 1036–1046, doi:10.2307/2269588, 1996. 5256
- 25 Gasche, R. and Papen, H.: A 3-year continuous record of nitrogen trace gas fluxes from untreated and limed soil of a N-saturated spruce and beech forest ecosystem in Germany – 2. NO and NO₂ fluxes, *J. Geophys. Res.-Atmos.*, 104, 18505–18520, doi:10.1029/1999JD900294, 1999. 5254
- Gelman, A., Carlin, J., Stern, H., and Rubin, D.: *Bayesian Data Analysis*, Chapman and Hall, 30 2 Edn., London, UK, 2003. 5250, 5256, 5257, 5268

UQ of soil GHG emissions using LandscapeDNDC

K.-H. Rahn et al.

Title Page

Abstract

Introduction

Conclusions

References

Tables

Figures



Back

Close

Full Screen / Esc

Printer-friendly Version

Interactive Discussion



UQ of soil GHG emissions using LandscapeDNDC

K.-H. Rahn et al.

[Title Page](#)
[Abstract](#)
[Introduction](#)
[Conclusions](#)
[References](#)
[Tables](#)
[Figures](#)
[Back](#)
[Close](#)
[Full Screen / Esc](#)
[Printer-friendly Version](#)
[Interactive Discussion](#)


- Gilks, W., Richardson, S., and Spiegelhalter, D.: Markov Chain Monte Carlo in Practice, Chapman and Hall, London, UK, 1996. 5254, 5257, 5262
- Grote, R., Lehmann, E., Brümmer, C., Brüggemann, N., Szarzynski, J., and Kunstmann, H.: Modelling and observation of biosphere-atmosphere interactions in natural savannah in Burkina Faso, West Africa, *Phys. Chem. Earth.*, 34, 251–260, doi:10.1016/j.pce.2008.05.003, 2009. 5253
- Grote, R., Kiese, R., Grünwald, T., Ourcival, J.-M., and Granier, A.: Modelling forest carbon balances considering tree mortality and removal, *Agr. Forest Meteorol.*, 151, 179–190, doi:10.1016/j.agrformet.2010.10.002, 2011. 5253
- Haas, E., Klatt, S., Fröhlich, A., Kraft, P., Werner, C., Kiese, R., Grote, R., Breuer, L., and Butterbach-Bahl, K.: Towards a new approach to simulating regional N₂O emissions – the LandscapeDNDC Model, *Landscape Ecol.*, accepted, LAND-11-3090, 2012. 5253
- Hamby, D. M.: A review of techniques for parameter sensitivity analysis of environmental models, *Environ. Monit. Assess.*, 32, 135–154, doi:10.1007/BF00547132, 1994. 5255
- Kass, R., Carlin, B., Gelman, A., and Neal, R.: Markov chain Monte Carlo in practice: a roundtable discussion, *Am. Stat.*, 52, 93–100, doi:10.2307/2685466, 1998. 5258, 5259
- Kesik, M., Ambus, P., Baritz, R., Brüggemann, N., Butterbach-Bahl, K., Damm, M., Duyzer, J., Horváth, L., Kiese, R., Kitzler, B., Leip, A., Li, C., Pihlatie, M., Pilegaard, K., Seufert, S., Simpson, D., Skiba, U., Smiatek, G., Vesala, T., and Zechmeister-Boltenstern, S.: Inventories of N₂O and NO emissions from European forest soils, *Biogeosciences*, 2, 353–375, doi:10.5194/bg-2-353-2005, 2005. 5253
- Kesik, M., Brüggemann, N., Forkel, R., Kiese, R., Knoche, R., Li, C., Seufert, G., Simpson, D., and Butterbach-Bahl, K.: Future scenarios of N₂O and NO emissions from European forest soils, *J. Geophys. Res.*, 111, 148–227, doi:10.1029/2005JG000115, 2006. 5251
- Kiese, R., Li, C., Hilbert, D., Papen, H., and Butterbach-Bahl, K.: Regional application of PnET-N-DNDC for estimating the N₂O source strength of tropical rainforests in the Wet Tropics of Australia, *Glob. Change Biol.*, 11, 128–144, doi:10.1111/j.1365-2486.2004.00873.x, 2005. 5251, 5252, 5253
- Klemedtsson, L., Jansson, P., Gustafsson, D., Karlberg, L., Weslien, P., von Arnold, K., Ernfors, M., Langvall, O., and Lindroth, A.: Bayesian calibration method used to elucidate carbon turnover in forest on drained organic soil, *Biogeochemistry*, 89, 61–79, 2008. 5252, 5256, 5264

UQ of soil GHG emissions using LandscapeDNDC

K.-H. Rahn et al.

Title Page

Abstract

Introduction

Conclusions

References

Tables

Figures

◀

▶

◀

▶

Back

Close

Full Screen / Esc

Printer-friendly Version

Interactive Discussion



- Lehuger, S., Gabrielle, B., van Oijen, M., Makowski, D., Germon, J., Morvan, T., and Hénault, C.: Bayesian-calibration of the nitrous oxide emission module of an agro-ecosystem model, *Agr. Ecosyst. Environ.*, 133, 208–222, 2009. 5252, 5256, 5264
- Li, C., Aber, J., Stange, F., Butterbach-Bahl, K., and Papen, H.: A process-oriented model of N₂O and NO emissions from forest soils: 1. model development, *J. Geophys. Res.-Atmos.*, 105, 4369–4384, doi:10.1029/1999JD900949, 2000. 5253
- Li, C., Zhuang, Y., Cao, M., Crill, P., Dai, Z., Frohking, S., Moore III, B., Salas, W., Song, W., and Wang, X.: Comparing a process-based agro-ecosystem model to the IPCC methodology for developing a national inventory of N₂O emissions from arable lands in China, *Nutr. Cycl. Agroecosys.*, 60, 159–175, 2001. 5253
- Li, C., Mosier, A., Wassmann, R., Cai, Z., Zheng, X., Huang, Y., Tsuruta, H., Boonjawat, J., and Lantin, R.: Modeling greenhouse gas emissions from rice-based production systems: Sensitivity and upscaling, *Global Biogeochem. Cy.*, 18, GB1043, doi:10.1029/2003GB002045, 2004. 5251, 5252
- Metropolis, N., Rosenbluth, A. W., Rosenbluth, M. N., Teller, A. H., and Teller, E.: Equation of state calculations by fast computing machines, *J. Chem. Phys.*, 21, 1087–1092, 1953. 5257
- Morris, M. D.: Factorial sampling plans for preliminary computational experiments, *Technometrics*, 33, 161–174, available online: <http://www.jstor.org/stable/1269043>, 1991. 5254
- van Oijen, M., Rougier, J., and Smith, R.: Bayesian calibration of process-based forest models: bridging the gap between models and data, *Tree Physiol.*, 25, 915–927, 2005. 5252, 5256, 5257, 5264
- van Oijen, M., Cameron, D., Butterbach-Bahl, K., Farahbakhshazad, N., Jansson, P.-E., Kiese, R., Rahn, K.-H., Werner, C., and Yeluripati, J.: A Bayesian framework for model calibration, comparison and analysis: application to four models for the biogeochemistry of a Norway spruce forest, *Agr. Forest Meteorol.*, doi:10.1016/j.agrformet.2011.06.017, 2011. 5252, 5254, 5255, 5265
- Papen, H. and Butterbach-Bahl, K.: A 3-year continuous record of nitrogen trace gas fluxes from untreated and limed soil of a N-saturated spruce and beech forest ecosystem in Germany - 1. N₂O emissions, *J. Geophys. Res.-Atmos.*, 104, 18487–18503, doi:10.1029/1999JD900293, 1999. 5254, 5263, 5266
- Pathak, H., Li, C., and Wassmann, R.: Greenhouse gas emissions from Indian rice fields: calibration and upscaling using the DNDC model, *Biogeosciences*, 2, 113–123, doi:10.5194/bg-2-113-2005, 2005. 5251

UQ of soil GHG emissions using LandscapeDNDC

K.-H. Rahn et al.

[Title Page](#)
[Abstract](#)
[Introduction](#)
[Conclusions](#)
[References](#)
[Tables](#)
[Figures](#)
[Back](#)
[Close](#)
[Full Screen / Esc](#)
[Printer-friendly Version](#)
[Interactive Discussion](#)


Potter, C., Matson, P., Vitousek, P., and Davidson, E.: Process modeling of controls on nitrogen trace gas emissions from soils worldwide, *J. Geophys. Res.-Atmos.*, 101, 1361–1377, doi:10.1029/95JD02028, 1996. 5251

Rahn, K.-H., Butterbach-Bahl, K., and Werner, C.: Selection of likelihood parameters for complex models determines the effectiveness of Bayesian calibration, *Ecol. Inform.*, doi:10.1016/j.ecoinf.2011.08.002, 2011. 5258, 5265, 5267

Refsgaard, J. C., van der Sluijs, J. P., Brown, J., and van der Keur, P.: A framework for dealing with uncertainty due to model structure error, *Adv. Water Resour.*, 29, 1586–1597, doi:10.1016/j.advwatres.2005.11.013, available online: <http://www.sciencedirect.com/science/article/pii/S0309170805002903>, 2006. 5252

Reinds, G. J., van Oijen, M., Heuvelink, G. B., and Kros, H.: Bayesian calibration of the VSD soil acidification model using European forest monitoring data, *Geoderma*, 146, 475–488, 2008. 5256

Salas, W., Boles, S., Li, C., Yeluripati, J. B., Xiao, X., Frolking, S., and Green, P.: Mapping and modelling of greenhouse gas emissions from rice paddies with satellite radar observations and the DNDC biogeochemical model, *Aquat. Conserv.*, 17, 319–329, doi:10.1002/aqc.837, 2007. 5251

Saltelli, A. (Ed.): *Global Sensitivity Analysis: the Primer*, Wiley, Chichester, West Sussex, 2008. 5254

Stange, F., Butterbach-Bahl, K., Papen, H., Zechmeister-Boltenstern, S., Li, C., and Aber, J.: A process-oriented model of N₂O and NO emissions from forest soils. 2. sensitivity analysis and validation, *J. Geophys. Res.-Atmos.*, 105, 4385–4398, doi:10.1029/1999JD900948, 2000. 5253, 5267

Svensson, M., Jansson, P.-E., Gustafsson, D., Kleja, D. B., Langvall, O., and Lindroth, A.: Bayesian calibration of a model describing carbon, water and heat fluxes for a Swedish boreal forest stand, *Ecol. Model.*, 213, 331–344, 2008. 5252, 5264

Toft, N., Innocent, G. T., Gettinby, G., and Reid, S. W.: Assessing the convergence of Markov Chain Monte Carlo methods: an example from evaluation of diagnostic tests in absence of a gold standard, *Prev. Vet. Med.*, 79, 244–256, doi:10.1016/j.prevetmed.2007.01.003, 2007. 5259

Vrugt, J. A., Gupta, H. V., Bouten, W., and Sorooshian, S.: A Shuffled Complex Evolution Metropolis algorithm for optimization and uncertainty assessment of hydrologic model parameters, *Water Resour. Res.*, 39, 1201, doi:10.1029/2002WR001642, 2003. 5252, 5254

UQ of soil GHG emissions using LandscapeDNDC

K.-H. Rahn et al.

Title Page

Abstract

Introduction

Conclusions

References

Tables

Figures

◀

▶

◀

▶

Back

Close

Full Screen / Esc

Printer-friendly Version

Interactive Discussion



Vrugt, J. A., ter Braak, C. J. F., Clark, M. P., Hyman, J. M., and Robinson, B. A.: Treatment of input uncertainty in hydrologic modeling: Doing hydrology backward with Markov chain Monte Carlo simulation, *Water Resour. Res.*, 44, W00B09, doi:10.1029/2007WR006720, 2008. 5251

5 Vrugt, J. A., ter Braak, C. J. F., Diks, C. G. H., Robinson, B. A., Hyman, J. M., and Higdon, D.: Accelerating Markov chain Monte Carlo simulation by differential evolution with self-adaptive randomized subspace sampling, *Int. J. Nonlin. Sci. Num.*, 10, 273–290, 2009. 5260, 5265

Werner, C., Zheng, X., Tang, J., Xie, B., Liu, C., Kiese, R., and Butterbach-Bahl, K.: N₂O, CH₄ and CO₂ emissions from seasonal tropical rainforests and a rubber plantation in Southwest China, *Plant Soil*, 289, 335–353, doi:10.1007/s11104-006-9143-y, 2006. 5251

10 Werner, C., Butterbach-Bahl, K., Haas, E., Hickler, T., and Kiese, R.: A global inventory of N₂O emissions from tropical rainforest soils using a detailed biogeochemical model, *Global Biogeochem. Cy.*, 21, GB3010, doi:10.1029/2006GB002909, 2007. 5252, 5253

Wikle, C.: Hierarchical Bayesian models for predicting the spread of ecological processes, *Ecology*, 84, 1382–1394, doi:10.1890/0012-9658(2003)084[1382:HBMFPT]2.0.CO;2, 2003. 5251

Winiwarter, W. and Rypdal, K.: Assessing the uncertainty associated with national greenhouse gas emission inventories: a case study for Austria, *Atmos. Environ.*, 35, 5425–5440, doi:10.1016/S1352-2310(01)00171-6, available online: <http://www.sciencedirect.com/science/article/pii/S1352231001001716>, 2001. 5252

20 Wolf, B., Zheng, X., Brüggemann, N., Chen, W., Dannenmann, M., Han, X., Sutton, M. A., Wu, H., Yao, Z., and Butterbach-Bahl, K.: Grazing-induced reduction of natural nitrous oxide release from continental steppe, *Nature*, 464, 881–884, doi:10.1038/nature08931, 2010. 5263, 5266

25 Wolf, B., Chen, W., Brüggemann, N., Zheng, X., Pumpanen, J., and Butterbach-Bahl, K.: Applicability of the soil gradient method for estimating soil-atmosphere CO₂, CH₄, and N₂O fluxes for steppe soils in Inner Mongolia, *J. Plant Nutr. Soil Sc.*, 174, 359–372, doi:10.1002/jpln.201000150, 2011. 5267

30 Wu, X., Brüggemann, N., Gasche, R., Shen, Z., Wolf, B., and Butterbach-Bahl, K.: Environmental controls over soil-atmosphere exchange of N₂O, NO, and CO₂ in a temperate Norway spruce forest, *Global Biogeochem. Cy.*, 24, GB2012, doi:10.1029/2009GB003616, 2010. 5253

Table 1. Selected parameters being most influential for simulating soil-atmosphere trace gas fluxes (N₂O, NO and CO₂) with LandscapeDNDC.

| Parameter | Description |
|-------------|---|
| D_N2O | effective N ₂ O diffusion constant [m ² h ⁻¹] |
| D_NO | effective NO diffusion constant [m ² h ⁻¹] |
| DRF | scaling factor for decomposition rate constants of SOM |
| EFFAC | partitioning of CO ₂ and DOC production during microbial decomposition of organic matter |
| FNO3.U | fraction of microbial N-uptake as (NO ₃) |
| FRC | factor regulating microbial death depending on the availability of very labile and labile carbon |
| FTRANS | factor regulating microbial nitrate immobilisation and direct re-mineralisation to NH ₄ |
| KCRB.L | decomposition constant of labile dead microbial biomass |
| KHDC.L | decomposition constant of labile humads |
| KHDC.R | decomposition constant of recalcitrant humads |
| KM.O2 | factor regulating splitting of DOC and CO ₂ during decomposition of SOM depending on O ₂ concentration |
| KMDC.DOC | factor for half optimum content of doc in soil solution for denitrifier activity [kgCha ⁻¹] |
| KMDC.N | factor for half optimum content of nitrogen in soil solution for denitrifier activity [kgNha ⁻¹] |
| KMM.DOC | factor regulating growth of microbes in dependency of DOC substrate |
| KMNO2 | factor regulating NO ₂ to NO ₃ conversion depending on NO ₂ concentration during nitrification |
| KN2O | loss rate of N ₂ O during nitrification |
| KNO | loss rate of NO during nitrification |
| KRCL | decomposition constant for labile litter pool |
| KRCR | decomposition constant for recalcitrant litter pool |
| MICRRESP | factor regulating CO ₂ production during microbial metabolism in dependency of microbial C/N ratio |
| NH4.DENIMAX | maximum fraction of NH ₄ available for auto- and heterotrophic nitrification |
| PERTL | fraction of labile litter, which can be reallocated into deeper soil layers |
| PERTR | fraction of recalcitrant litter, which can be reallocated into deeper soil layers |
| PERTVL | fraction of very labile litter, which can be reallocated into deeper soil layers |
| PSL.SC | depth dependent factor for reallocation of organic matter into deeper soil layers |
| SRB | fraction of labile dead microbial biomass |

UQ of soil GHG emissions using LandscapeDNDC

K.-H. Rahn et al.

Title Page

Abstract Introduction

Conclusions References

Tables Figures

◀ ▶

◀ ▶

Back Close

Full Screen / Esc

Printer-friendly Version

Interactive Discussion



Table 2. Summary of marginal parameter distribution. Posterior SD and skewness were estimated whereas the prior SD was analytically calculated.

| Parameter | θ_{MAP} | 95 % cred. interval | description | SD _{prior} | SD _{post} | $\frac{SD_{post}}{SD_{prior}}$ | skewness |
|-------------|----------------|----------------------|-------------|---------------------|--------------------|--------------------------------|----------|
| D.N2O | 3.34e-03 | [0.001, 0.114] | right skew. | 0.043 | 0.027 | 0.62 | 2.78 |
| D.NO | 4.84e-02 | [0.018, 0.146] | flat | 0.04 | 0.039 | 0.95 | 0.17 |
| DRF | 5.49e-02 | [0.024, 0.055] | left skew. | 0.016 | 0.009 | 0.55 | -0.64 |
| EFFAC | 8.31e-01 | [0.290, 0.925] | bimodal | 0.192 | 0.205 | 1.00* | -0.21 |
| FNO3.U | 9.23e-01 | [0.428, 0.993] | left skew. | 0.18 | 0.153 | 0.85 | -1.77 |
| FRC | 2.74e-02 | [0.015, 0.381] | right skew. | 0.113 | 0.106 | 0.94 | 0.43 |
| FTRANS | 3.53e-02 | [6.69e-04, 0.048] | right skew. | 0.014 | 0.015 | 1.00* | 0.35 |
| KCRB.L | 3.22e+00 | [1.54, 3.92] | right skew. | 0.722 | 0.704 | 0.98 | 0.33 |
| KHDC.L | 2.89e-02 | [0.002, 0.029] | flat | 0.008 | 0.008 | 0.98 | -0.07 |
| KHDC.R | 2.20e-03 | [0.001, 0.015] | flat | 0.004 | 0.004 | 1.00* | -0.05 |
| KM.O2 | 1.13e-01 | [0.105, 0.950] | right skew. | 0.257 | 0.265 | 1.00* | 0.54 |
| KMDC.DOC | 8.25e-04 | [0.001, 0.025] | right skew. | 0.007 | 0.007 | 0.98 | 0.14 |
| KMDC.N | 5.53e-02 | [0.017, 0.230] | right skew. | 0.07 | 0.058 | 0.83 | 0.67 |
| KMM.DOC | 8.23e-03 | [3.17e-04, 0.009] | flat | 0.003 | 0.003 | 1.00* | 0.10 |
| KMNO2 | 4.13e-02 | [0.015, 0.069] | right skew. | 0.021 | 0.014 | 0.65 | 0.93 |
| KN2O | 1.01e-02 | [8.98e-04, 0.024] | right skew. | 0.026 | 0.006 | 0.23 | 1.71 |
| KNO | 9.53e-03 | [0.001, 0.024] | flat | 0.007 | 0.007 | 1.00* | -0.10 |
| KRCL | 2.20e-01 | [0.128, 0.888] | left skew. | 0.257 | 0.217 | 0.84 | -0.46 |
| KRCR | 2.65e-01 | [0.070, 0.298] | left skew. | 0.072 | 0.065 | 0.90 | -1.04 |
| MICRRSP | 5.06e-02 | [0.042, 0.118] | flat | 0.023 | 0.023 | 1.00* | -0.02 |
| NH4.DENIMAX | 8.21e-01 | [0.704, 0.966] | right skew. | 0.081 | 0.077 | 0.95 | 0.45 |
| PERTL | 6.38e-04 | [2.63e-04, 7.39e-04] | flat | 1.4e-04 | 1.4e-04 | 0.99 | -0.09 |
| PERTR | 8.53e-05 | [4.36e-05, 1.96e-04] | flat | 4.6e-05 | 4.7e-05 | 1.00 | 0.15 |
| PERTVL | 9.16e-03 | [8.15e-04, 0.015] | flat | 0.004 | 0.004 | 0.99 | 0.09 |
| PSL.SC | 1.21e-02 | [0.006, 0.029] | right skew. | 0.008 | 0.007 | 0.81 | 0.22 |
| SRB | 5.43e-01 | [0.512, 0.977] | flat | 0.141 | 0.14 | 0.99 | 0.04 |

* capped to 1.0.

UQ of soil GHG emissions using LandscapeDNC

K.-H. Rahn et al.

Title Page

Abstract

Introduction

Conclusions

References

Tables

Figures

◀

▶

◀

▶

Back

Close

Full Screen / Esc

Printer-friendly Version

Interactive Discussion



Table 3. Summary of cumulated measured and simulated emissions of NO, N₂O and CO₂. Simulated fluxes were only cumulated if corresponding periods with observations were available. Values in Brackets are calculated after freeze-thaw events.

| Soil flux | | 1994 | 1995 | 1996 | 1997 | 2002 | 2003 | Total | 2004 | 2005 | 2006 | 2007 | Total | |
|---|--|-------------|------------|------------|------------|------|------------|-------|------------|-------|------------|------------|-------|------------|
| NO [kgNha ⁻¹] | No of days | 357 | 341 | 350 | 359 | 275 | 208 | 1890 | 162 | 322 | 263 | 263 | 1010 | |
| | Minimum | 5.02 | 4.47 | 3.97 | 4.91 | 3.85 | 2.87 | | 1.78 | 3.88 | 2.88 | 3.61 | | |
| | Q _{0.005} | 5.95 | 5.33 | 4.79 | 5.71 | 4.52 | 3.34 | | 2.04 | 4.60 | 3.43 | 4.24 | | |
| | Mean | 7.31 | 6.55 | 5.94 | 7.12 | 5.50 | 4.39 | | 2.67 | 5.69 | 4.55 | 5.20 | | |
| | St. dev | 0.54 | 0.49 | 0.48 | 0.55 | 0.40 | 0.40 | | 0.27 | 0.44 | 0.44 | 0.39 | | |
| | Q _{0.995} | 8.75 | 7.87 | 7.30 | 8.56 | 6.55 | 5.40 | | 3.41 | 6.89 | 5.68 | 6.23 | | |
| | Maximum | 9.52 | 8.52 | 7.95 | 9.42 | 7.09 | 5.83 | | 3.86 | 7.61 | 6.35 | 6.82 | | |
| | Best | 7.05 | 6.42 | 5.91 | 6.75 | 5.50 | 4.23 | | 35.85 | 2.46 | 5.49 | 4.25 | 4.95 | 17.16 |
| | Measured | 6.23 | 8.16 | 8.69 | 6.98 | 4.24 | 6.73 | | 41.03 | 3.62 | 5.46 | 8.64 | 4.38 | 22.11 |
| | N ₂ O [kgNha ⁻¹] | No. of days | 345 | 358 | 343 | 346 | 343 | 340 | 2075 | 296 | 343 | 264 | 294 | 1197 |
| Minimum | | 0.33 | 0.30 | 0.23 | 0.29 | 0.28 | 0.23 | | 0.20 | 0.26 | 0.23 | 0.23 | | |
| Q _{0.005} | | 0.38 | 0.37 | 0.30 | 0.35 | 0.34 | 0.29 | | 0.25 | 0.32 | 0.28 | 0.27 | | |
| Mean | | 0.52 | 0.53 | 0.47 | 0.48 | 0.49 | 0.42 | | 0.36 | 0.45 | 0.38 | 0.38 | | |
| St. dev | | 0.06 | 0.06 | 0.07 | 0.05 | 0.06 | 0.06 | | 0.05 | 0.05 | 0.04 | 0.04 | | |
| Q _{0.995} | | 0.67 | 0.69 | 0.67 | 0.62 | 0.64 | 0.57 | | 0.50 | 0.60 | 0.51 | 0.49 | | |
| Maximum | | 0.76 | 0.83 | 0.78 | 0.72 | 0.75 | 0.69 | | 0.57 | 0.73 | 0.62 | 0.56 | | |
| Best | | 0.51 | 0.55(0.51) | 0.55(0.38) | 0.48(0.40) | 0.54 | 0.41(0.34) | | 3.02(2.68) | 0.37 | 0.45(0.37) | 0.39(0.3) | 0.39 | 1.60(1.43) |
| Measured | | 0.39 | 0.80(0.75) | 2.90(0.89) | 0.61(0.25) | 0.65 | 0.36(0.21) | | 5.72(3.29) | 0.16 | 0.97(0.74) | 2.14(0.51) | 0.47 | 3.74(1.88) |
| CO ₂ [kgCha ⁻¹] | | No. of days | | 287 | 355 | 362 | | | 1004 | 299 | 334 | 331 | 228 | 1192 |
| | Minimum | | 5584 | 4746 | 6404 | | | | 4607 | 5478 | 5434 | 3805 | | |
| | Q _{0.005} | | 6464 | 5590 | 7327 | | | | 5216 | 6314 | 6231 | 4387 | | |
| | Mean | | 7992 | 7074 | 9055 | | | | 6401 | 7844 | 7688 | 5436 | | |
| | St. dev | | 622 | 612 | 710 | | | | 498 | 625 | 600 | 436 | | |
| | Q _{0.995} | | 9591 | 8683 | 10918 | | | | 7706 | 9491 | 9265 | 6591 | | |
| | Maximum | | 10262 | 9354 | 11721 | | | | 8267 | 10176 | 9937 | 7081 | | |
| | Best | | 8133 | 7250 | 9282 | | | | 24665 | 6570 | 8036 | 7852 | 5576 | 28035 |
| | Measured | | 10673 | 8813 | 7740 | | | | 27226 | 5294 | 7332 | 7556 | 3913 | 24095 |

Title Page

Abstract

Introduction

Conclusions

References

Tables

Figures

◀

▶

◀

▶

Back

Close

Full Screen / Esc

Printer-friendly Version

Interactive Discussion



UQ of soil GHG emissions using LandscapeDNDC

K.-H. Rahn et al.

Table 4. Residual mean squared error (RMSE) per year and soil-atmosphere gas-flux for the best simulation (RMSE(θ_{MAP})) and the distribution of the gas-flux simulations. The minimal distance to the 99 % credible intervals was used to calculate the RMSE of the distribution (RMSE(CI)). Values in brackets are calculated using simulated emissions after freeze-thaw events.

| Soil flux | | 1994 | 1995 | 1996 | 1997 | 2002 | 2003 | 2004 | 2005 | 2006 | 2007 |
|---|------------------------|------|------------|-------------|------------|------|------------|--------|------------|------------|--------|
| NO [gNha ⁻¹ d ⁻¹] | No of days | 357 | 341 | 350 | 359 | 275 | 208 | 162 | 322 | 263 | 263 |
| | RMSE(CI) | 2.46 | 5.93 | 11.11 | 3.18 | 3.09 | 16.99 | 8.75 | 9.06 | 21.31 | 6.59 |
| | RMSE(θ_{MAP}) | 6.66 | 11.68 | 15.92 | 9.20 | 7.94 | 22.66 | 12.46 | 14.45 | 28.32 | 11.57 |
| N ₂ O [gNha ⁻¹ d ⁻¹] | No of days | 345 | 358 | 343 | 346 | 343 | 340 | 296 | 343 | 264 | 294 |
| | RMSE(CI) | 0.17 | 1.40(1.37) | 16.54(8.16) | 2.91(0.39) | 0.96 | 0.85(0.28) | 0.37 | 3.82(1.51) | 21.45(2.9) | 0.45 |
| | RMSE(θ_{MAP}) | 0.53 | 1.82(1.77) | 17.01(8.22) | 3.12(0.77) | 1.45 | 1.09(0.67) | 0.83 | 4.19(2.17) | 21.80(3.1) | 1.06 |
| CO ₂ [gCha ⁻¹ d ⁻¹] | No of days | | 287 | 355 | 362 | | | 299 | 334 | 331 | 228 |
| | RMSE(CI) | | 10 680 | 6694 | 5804 | | | 8991 | 10 311 | 12 483 | 12 644 |
| | RMSE(θ_{MAP}) | | 15 344 | 9986 | 8989 | | | 11 623 | 13 106 | 15 806 | 16 446 |

Title Page

Abstract Introduction

Conclusions References

Tables Figures

◀ ▶

◀ ▶

Back Close

Full Screen / Esc

Printer-friendly Version

Interactive Discussion



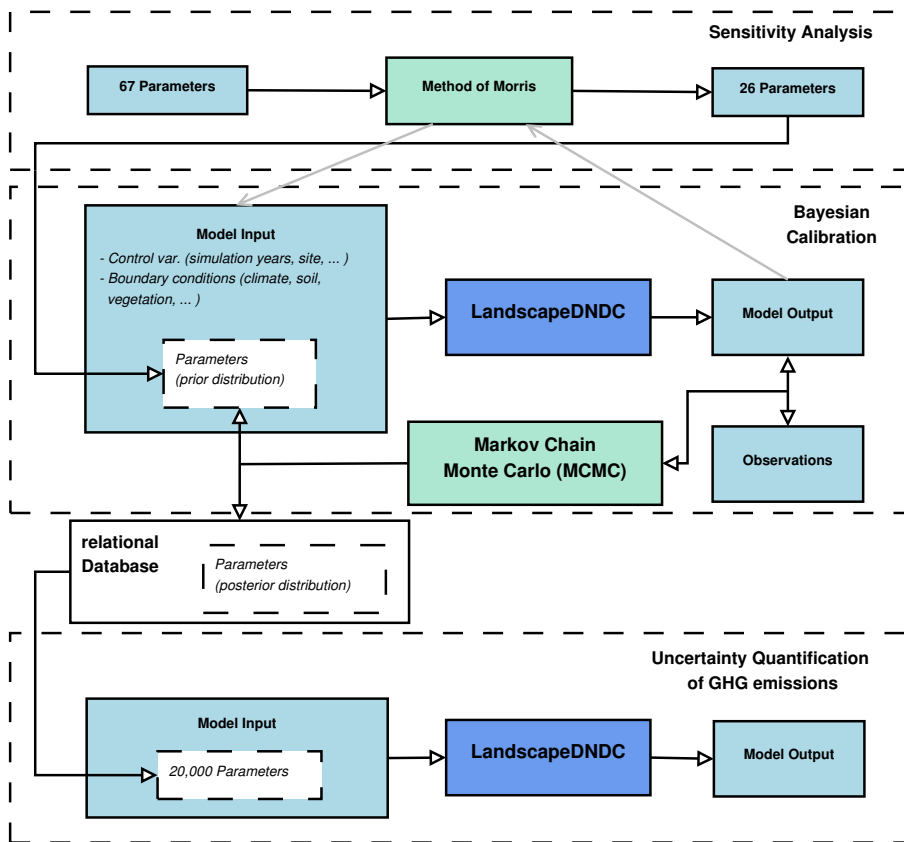


Fig. 1. Schematic view of the workflow for assessing the uncertainty of simulated soil GHG emissions while using LandscapeDNDC. After reduction to influential parameters by means of a sensitivity analysis, the distribution of the model parameters was estimated using a Bayesian calibration. Subsequently, an uncertainty quantification of simulated emissions was carried out using 20 000 samples out of the 200 000 post burn-in realisations of the parameter distribution stored in a relational database.

Title Page

Abstract Introduction

Conclusions References

Tables Figures

◀ ▶

◀ ▶

Back Close

Full Screen / Esc

Printer-friendly Version

Interactive Discussion

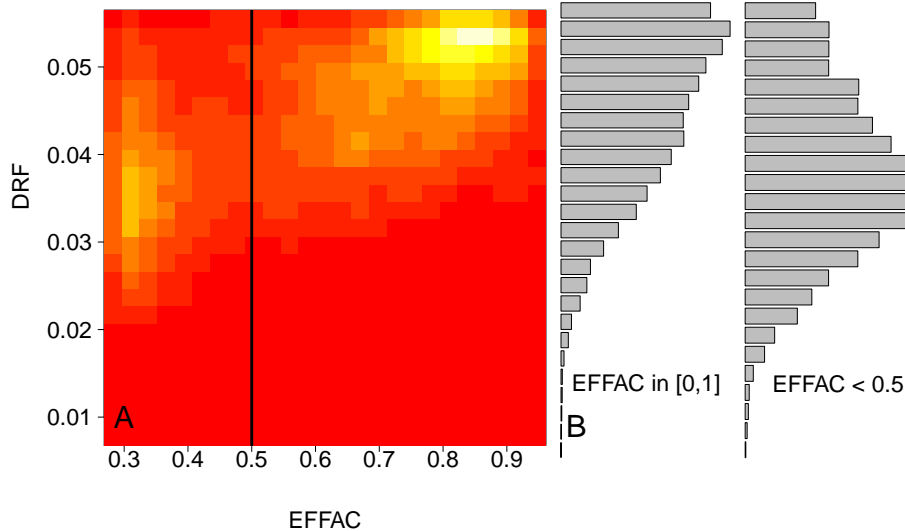


Fig. 2. A: Heat-map of 2-dimensional marginal distribution of EFFAC and DRF (decomposition rate factor), the brighter the polygons, the higher the posterior value. **B:** histogram of DRF using all values and histogram of DRF using only values of DRF, where EFFAC < 0.5.

UQ of soil GHG emissions using LandscapeDNDC

K.-H. Rahn et al.

Title Page

Abstract Introduction

Conclusions References

Tables Figures

◀ ▶

◀ ▶

Back Close

Full Screen / Esc

Printer-friendly Version

Interactive Discussion



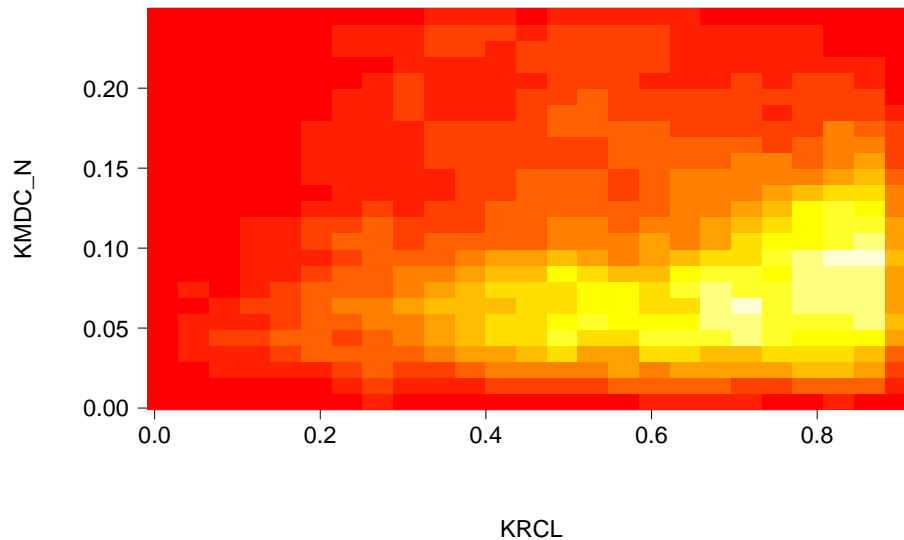


Fig. 3. Heat-map of 2-dimensional marginal distribution of KRCL (decomposition constant for labile litter pool) and KMDC_N (factor for half optimum content of nitrogen in soil solution for denitrifier activity). Higher values of KRCL lead to a wider range of KMDC_N.

UQ of soil GHG emissions using LandscapeDNDC

K.-H. Rahn et al.

Title Page

Abstract Introduction

Conclusions References

Tables Figures

◀ ▶

◀ ▶

Back Close

Full Screen / Esc

Printer-friendly Version

Interactive Discussion



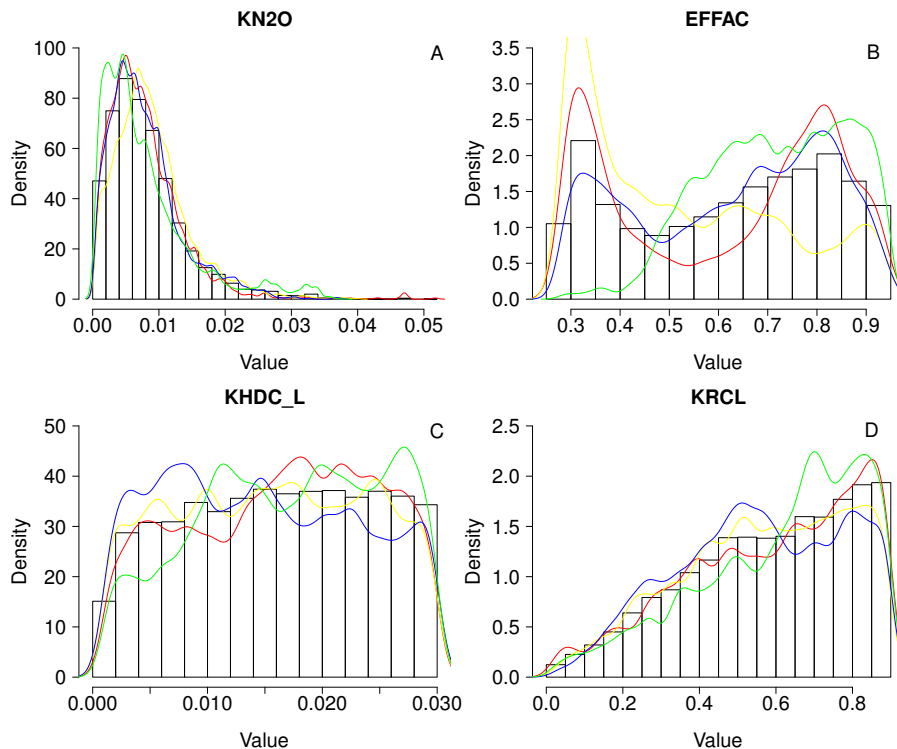


Fig. 4. Four typical histograms of marginal parameter distributions. The coloured density lines of a right-skewed (KN2O: loss rate of N₂O during nitrification), bi-modal (EFFAC: describing the partitioning of CO₂ and DOC production during microbial decomposition of organic matter), flat (KHDC_L: decomposition constant of labile humads pool) and a left-skewed distribution (KRCL: decomposition constant of labile litter pool) were done by post burn-in samples of each individual chain, whereas the histograms are plotted using post burn-in samples of all chains.

Title Page

Abstract

Introduction

Conclusions

References

Tables

Figures

◀

▶

◀

▶

Back

Close

Full Screen / Esc

Printer-friendly Version

Interactive Discussion



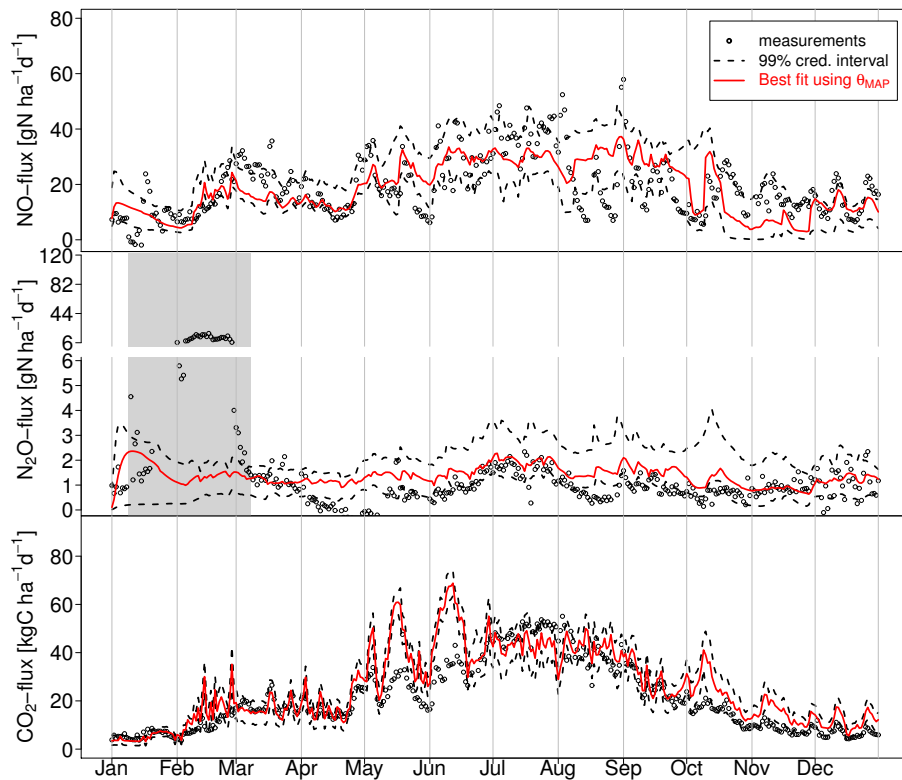


Fig. 5. Simulated fluxes (calibration set) versus measurements of NO, N₂O and CO₂ fluxes at the spruce site of the Höglwald Forest in the year 1997. The grey box highlights pulse emissions of N₂O during soil freeze-thaw events.

UQ of soil GHG emissions using LandscapeDNDC

K.-H. Rahn et al.

Title Page

Abstract

Introduction

Conclusions

References

Tables

Figures

◀

▶

◀

▶

Back

Close

Full Screen / Esc

Printer-friendly Version

Interactive Discussion



UQ of soil GHG emissions using LandscapeDNDC

K.-H. Rahn et al.

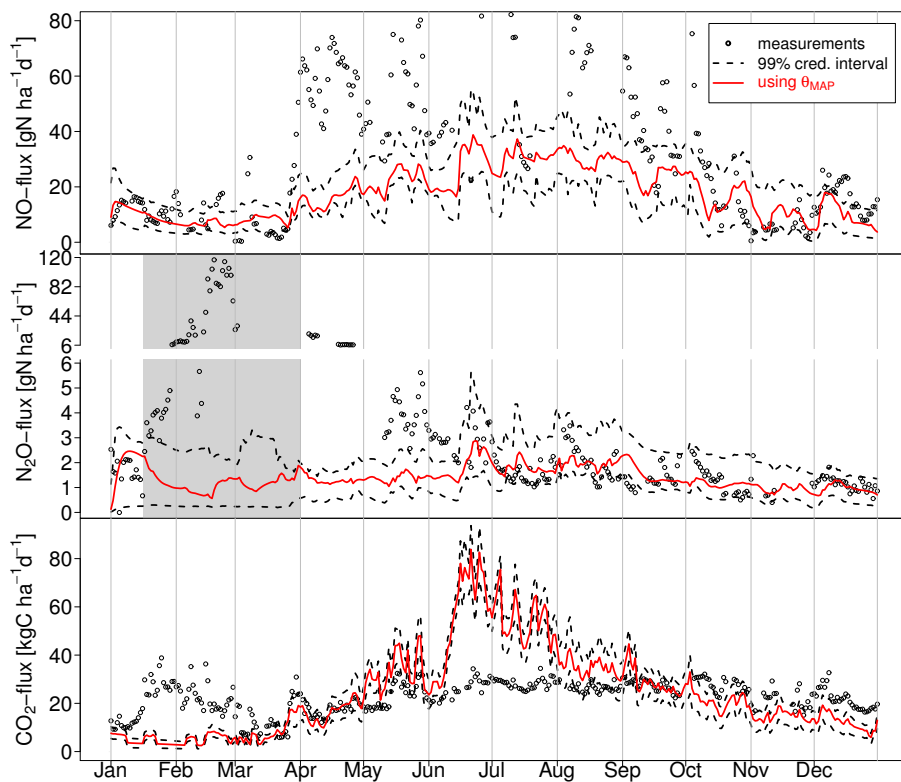


Fig. 6. Simulated fluxes (validation set) versus measurements of NO, N₂O and CO₂ fluxes at the spruce site of the Höglwald Forest in the year 2006. The grey box highlights pulse emissions of N₂O during soil freeze-thaw events.

[Title Page](#)[Abstract](#)[Introduction](#)[Conclusions](#)[References](#)[Tables](#)[Figures](#)[◀](#)[▶](#)[◀](#)[▶](#)[Back](#)[Close](#)[Full Screen / Esc](#)[Printer-friendly Version](#)[Interactive Discussion](#)

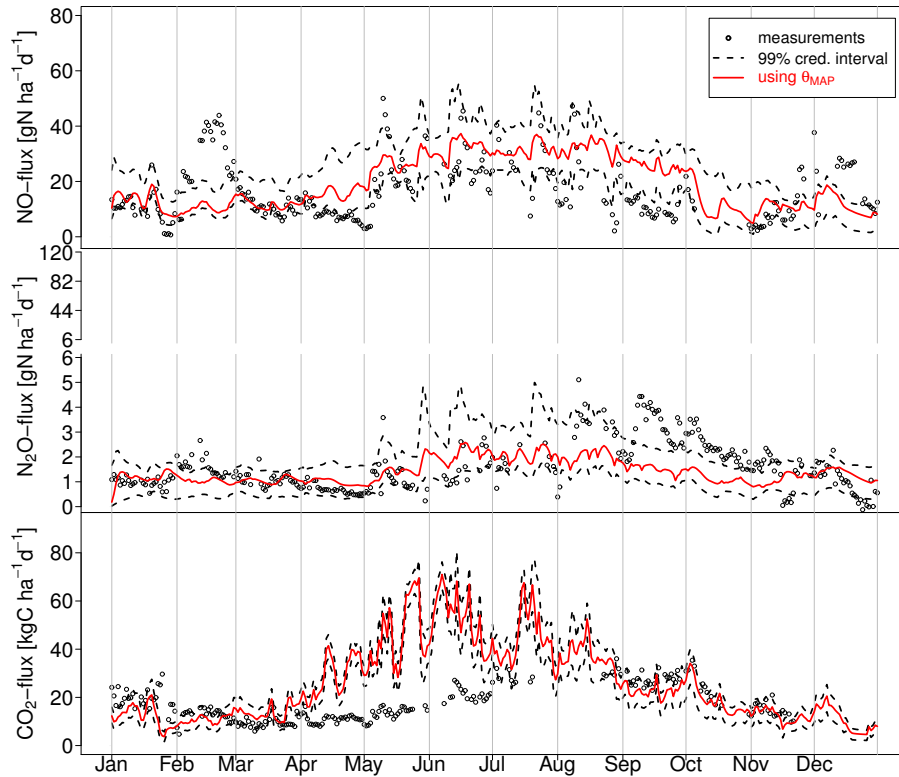


Fig. 7. Simulated fluxes (validation set) versus measurements of NO, N₂O and CO₂ fluxes at the spruce site of the Höglwald Forest in the year 2007.

UQ of soil GHG emissions using LandscapeDNDC

K.-H. Rahn et al.

Title Page

Abstract

Introduction

Conclusions

References

Tables

Figures

◀

▶

◀

▶

Back

Close

Full Screen / Esc

Printer-friendly Version

Interactive Discussion



UQ of soil GHG emissions using LandscapeDNDC

K.-H. Rahn et al.

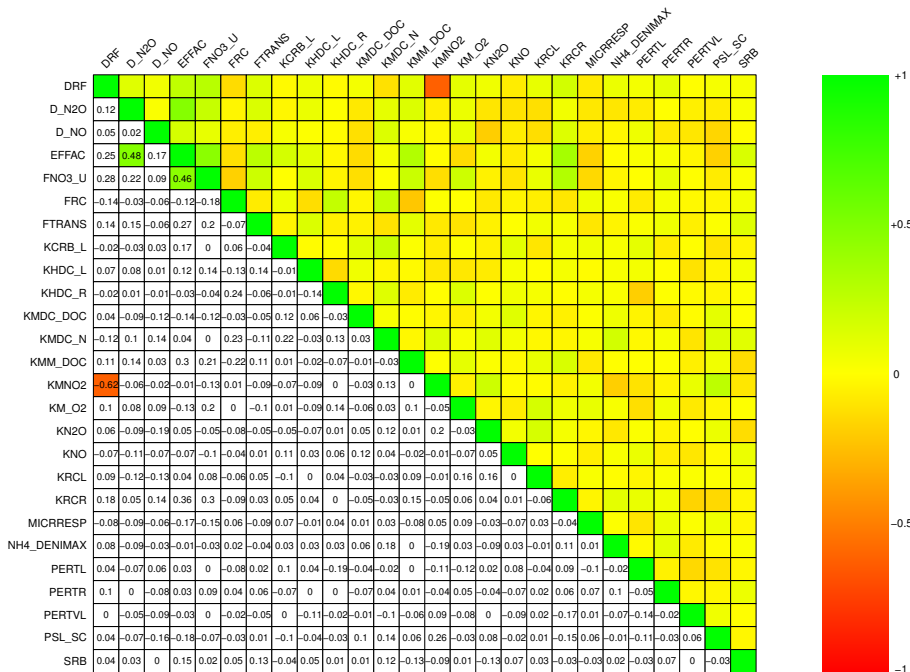


Fig. 8. Correlations of all 200 000 post burn-in parameter samples.

Title Page

Abstract Introduction

Conclusions References

Tables Figures

◀ ▶

◀ ▶

Back Close

Full Screen / Esc

Printer-friendly Version

Interactive Discussion



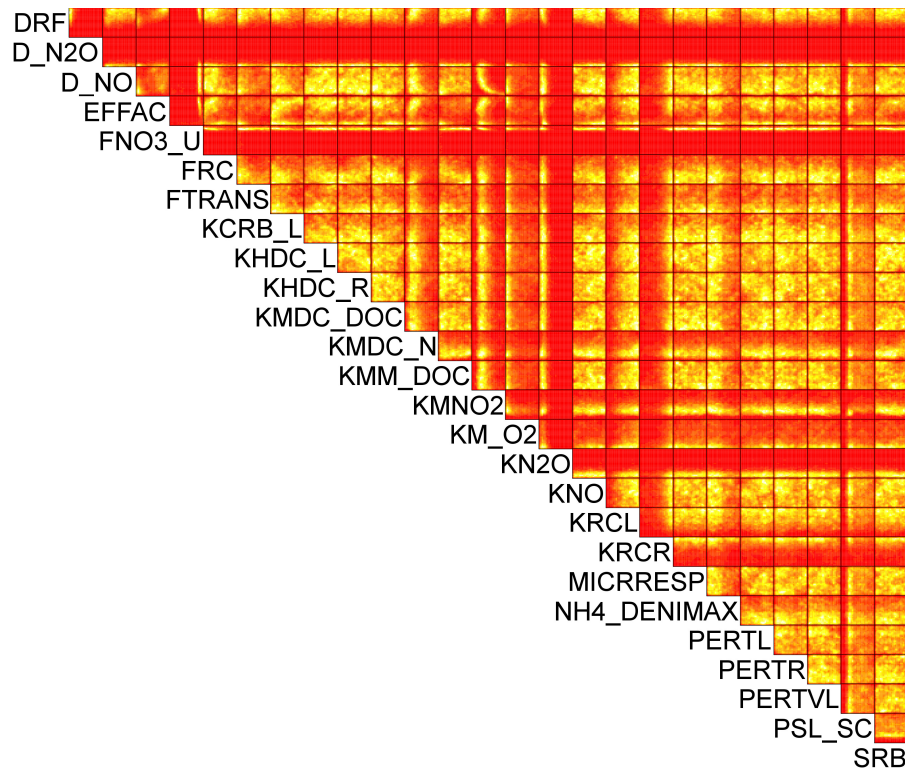


Fig. 9. Heat-maps of pair-wise marginal distributions; brighter polygons show higher posterior values.

UQ of soil GHG emissions using LandscapeDNC

K.-H. Rahn et al.

Title Page

Abstract Introduction

Conclusions References

Tables Figures

◀ ▶

◀ ▶

Back Close

Full Screen / Esc

Printer-friendly Version

Interactive Discussion

